AIMS Mathematics, 8(3): 5670–5686.
DOI: 10.3934/math.2023285
Received: 04 October 2022
Revised: 08 December 2022
Accepted: 13 December 2022
Published: 22 December 2022

http://www.aimspress.com/journal/Math

Research article

Investigation of chaotic behavior and adaptive type-2 fuzzy controller approach for Permanent Magnet Synchronous Generator (PMSG) wind turbine system

Aceng Sambas[1,4], Ardashir Mohammadzadeh[2], Sundarapandian Vaidyanathan[3], Ahmad Faisal Mohamad Ayob[4], Amiral Aziz[5], Mohamad Afendee Mohamed[6,*], Ibrahim Mohammed Sulaiman[7] and Mohamad Arif Awang Nawi[8,*]

[1] Department of Mechanical Engineering, Universitas Muhammadiyah Tasikmalaya, Tasikmalaya, Jawa Barat 46196, Indonesia
[2] Electrical Engineering Department, University of Bonab, Bonab, Iran
[3] Centre for Control Systems, Vel Tech University, Vel Nagar, Avadi, Chennai 600 062, Tamil Nadu
[4] Faculty of Ocean Engineering Technology and Informatics, Universiti Malaysia Terengganu, Malaysia
[5] Research Center for Conversion and Conservation Energy-National Research and Innovation Agency Republic of Indonesia (BRIN), South Tangerang 15314, Indonesia
[6] Faculty of Informatics and Computing, Universiti Sultan Zainal Abidin, Terengganu, Malaysia
[7] School of Quantitative Sciences, Universiti Utara Malaysia, Sintok, Kedah 06010, Malaysia
[8] School of Dental Sciences, Health Campus, Universiti Sains Malaysia, Kelantan 16150, Malaysia

* **Correspondence:** Email: mafendee@unisza.edu.my, mohamadarif@usm.my.

Abstract: This article begins with a dynamical analysis of the Permanent Magnet Synchronous Generator (PMSG) in a wind turbine system with quadratic nonlinearities. The dynamical behaviors of the PMSG are analyzed and examined using Poincare map, bifurcation model, and Lyapunov spectrum. Finally, an adaptive type-2 fuzzy controller is designed for different flow configurations of the PMSG. An analysis of the performance for the proposed approach is evaluated for effectiveness by simulating the PMSG. In addition, the proposed controller uses advantages of adaptive type-2 fuzzy controller in handling dynamic uncertainties to approximate unknown non-linear actions.

Keywords: chaotic system; PMSG; dynamical analysis; turbine; adaptive type-2 fuzzy controller

Mathematics Subject Classification: 34A07, 34A34, 34H10, 34K23

1. Introduction

Recently, the amount of wind energy produced has increased at a quicker rate in order to safeguard the environment from pollution by reducing the reliance on fossil fuel [1,2]. Different categories of generators such as PMSG [3,4], Squirrel Cage Induction generators (SCIG) [5,6], multi-phase induction generator (MPIG) [7,8], doubly salient electromagnetic generator (DSEG) [9,10] and double feed induction generator (DFIG) [11,12], can be employed by the wind turbine to produce electrical energy.

The effective utilization of wind turbines, which transforms wind mechanical energy into useful electrical energy has led to significant application of physics in this area [13]. Particularly, the use of PMSG in wind turbine exhibit significant advantages in terms of high efficiency and low maintenance [14,15]. Based on this, many studies have been directed towards the control of PMSG [16–20].

Several investigations have shown that PMSG produces chaotic behavior that can be well controlled. For instance, Ren et al. [21] investigated the dynamic motion of the wind turbine PMSG using optimal control theory. The authors demonstrated the efficiency of the control system. Messadi et al. [22] addressed the problem of optimality of angle and speed of the turbine blade in PMSG using predictive control approach with the purpose of generating the maximum power. Si et al. [23] proposed a delayed feedback control PMSG model of a wind turbine in fractional-order and an extensive study in terms of non-linear dynamics were conducted. The study demonstrated how the parameters of different system can influence the control result of the system. A sliding mode control approach using state feedback on a PMSG was presented by Alamdar and Balochian [24]. The authors discovered that the controller can monitor any desired point and can further converge a chaotic system to zero. Hu et al. [25] investigated an adaptive control approach integrating the type-2 sequential fuzzy neural network (T2SFNN) and chaotic motion for the PMSG. The authors illustrated how the control strategy can tame chaos by demonstrating the effectiveness of the strategy. For the PMSG-based wind energy conversion system, Kahla et al. [26] proposed the maximum power extraction frameworks operating the cutting-edge optimization approaches using the feedback linearization control strategy and the fractional control theory. They demonstrated the efficacy of the suggested 3-kW PMSG control system, based on a wind energy conversion technology. An event-triggered neural adaptative backstepping control approach for the K chaotic PMSG coupled system was presented in Luo et al. [27] The study discovered that the Lyapunov function proves the stability of the suggested scheme, and simulation results demonstrated the efficiency of the method.

Recently, the topic of chaotic Permanent Magnet Synchronous Generator (PMSG) based the conversion system of wind energy has been studied intensively. Takhi et al. [28] studied the problem of control and synchronization of the chaotic PMSG system which contains perturbations and uncertainties using predictive control. The authors further applied Arduino boards to verify the approach via microcontroller implementation. Dursun et al. [29] presented maximum power extraction frameworks operating the state-of-the-art optimization methods for permanent magnet synchronous generator (PMSG). This was achieved using the wind energy conversion system (WECS). Shanmugam and Joo [30] investigated the stabilization analysis for nonlinear permanent magnet synchronous

generator (PMSG)-based wind turbine system under fuzzy-based memory sampled-data (FBMSD) control scheme.

To the best of our knowledge, the adaptive type-2 fuzzy controller in the chaotic PMSG model has not been studied. Therefore, due to its effectiveness and performance, this study tends to investigate the Adaptive Type-2 Fuzzy Controller method for controlling the chaotic PMSG based on the conversion system of wind energy.

With regard to the aforementioned discussions, we highlight the main contribution and the novelty of this study are as follows:

a) Investigating chaotic behavior in the PMSG based on the wind turbine system using Lyapunov spectrum, bifurcation model, Poincare map, and complexity theory.
b) This work further studied the mathematical model and numerical simulation of the adaptive type-2 fuzzy controller for chaotic PMSG a wind turbine system.

The other parts of this study are structured as follows. Section 2 present the mathematical model of the PMSG based on the wind turbine system. Section 3 investigate the nonlinear dynamics of PMSG based on different system orders. Section 4 present an adaptive type-2 fuzzy controller of the PMSG model. Finally, Section 5 concludes the findings of this paper.

2. Modeling and formulation of the PMSG systems

This section will discuss about the mathematical model of PMSG based on selected wind conversion system (see Figure 1). The back-to-back converter employed for transporting power generated by the generator to the grid is where the adaptive type-2 fuzzy controller is primarily focused.

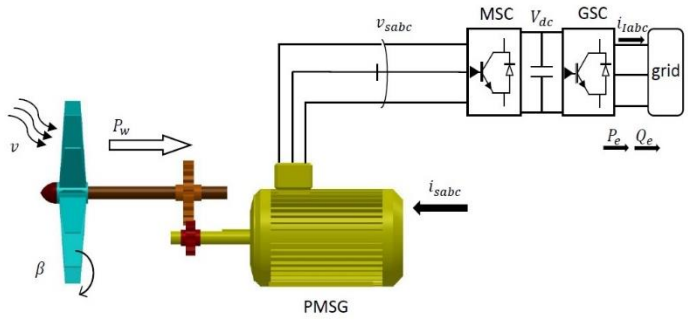

Figure 1. The configuration of a PMSG wind turbine.

The parameters description will be presented as follows [22]:

V : Wind;
MSC : Machine-side converter;
V_{dc} : Dc-link voltage;
i_{sabc} : Stator three-phase current;
u_{sabc} : Stator three-phase voltage;
β : Pitch angle;
GSC : Grid side converter;
Pe : The active output power;

P_w : The power extracted from the wind;
i_{labs} : Load current;
Qe : The reactive output power.

According to [22], the mathematical model for PMSG following rotor coordinate system can be given as in (1):

$$\begin{cases} \frac{dw}{dt'} = \frac{P}{J}\left(\phi_f i_q + \left(L_d - L_q\right) i_d i_q\right) - \frac{f}{J} w - \frac{T_1}{J}, \\ \frac{di_q}{dt'} = -\frac{R_s}{L_q} i_q + \frac{L_d}{L_q} p w i_d - \frac{p\phi_f}{L_q} w + \frac{u_q}{L_d}, \\ \frac{di_d}{dt'} = -\frac{R_s}{L_d} i_d + \frac{L_q}{L_d} p w i_q + \frac{u_d}{L_d}, \end{cases} \tag{1}$$

The variables description will be presented as follows:

$\{i_q,i_d\},\{u_q,u_d\},\{L_q,L_d\}$: currents, voltages and inductance of quadrature and direct axis stator in pairs;

t' : Time;
f : Viscous friction coefficient;
J : Rotor moment of inertia;
T_1 : Load torque;
ϕ_f : Rotor magnet flux linking the stator;
R_s : Stator resistance;
p : Number of poles pairs.

The simplified form of Eq (1) can be obtained by transforming the affine and time scaling as follows [22]:

$$\begin{cases} \frac{d\tilde{w}}{dt} = \sigma\left(\tilde{\imath}_q - \tilde{w}\right) + \varepsilon \tilde{\imath}_d \tilde{\imath}_q\right) - \tilde{T}, \\ \frac{d\tilde{\imath}_q}{dt} = -\tilde{\imath}_q - \tilde{w}\tilde{\imath}_d + \gamma \tilde{w} + \tilde{u}_q, \\ \frac{di_d}{dt} = -\tilde{\imath}_d + \tilde{w}\tilde{\imath}_q + \tilde{u}_d, \end{cases} \tag{2}$$

with $\sigma = \frac{fL_q}{R_s J}$, $\varepsilon = \frac{pbL_q^2 k^2 (L_q - L_d)}{JR_s^2}$, $\gamma = -\frac{\phi_f}{kL_q}$, $b = \frac{L_q}{L_d}$, $k = \frac{fR}{L_q p \phi_f}$, $\tilde{\imath}_d = \frac{L_d p \phi_f}{f R_s} i_d$, $\tilde{\imath}_q = \frac{L_q p \phi_f}{f R_s} i_q$, $\tilde{w} = \frac{L_q}{R_s} w$, $\tilde{u}_d = \frac{1}{R_s k} u_d$, $\tilde{u}_d = \frac{1}{R_s k} u_d$, $\tilde{u}_q = \frac{1}{R_s k} u_q$, $\tilde{T} = \frac{L_q^2}{JR_s^2} T_1$ and $t = \frac{R_s t'}{L_q}$.

The state vector y assumes the forms $y = \left[w, i_q, i_d\right]^T$ and the PMSG model in Eq (2) is transformable to the normalized PMSG model [22]:

$$\begin{cases} \dot{y}_1 = a(y_2 - y_1) + \tilde{T} + y_3 y_2, \\ \dot{y}_2 = -y_2 - y_1 y_3 + b y_1 + \tilde{u}_q, \\ \dot{y}_3 = -y_3 + y_1 y_2 + \tilde{u}_d, \end{cases} \tag{3}$$

where *a* and *b* denote the operating parameters. The PMSG exhibits chaotic behavior by limiting the values of *a* and *b* into certain boundary and setting the external parameters to zero, that is, $\tilde{T} = \tilde{u}_q = \tilde{u}_d = 0$. Then Eq (3) become

$$\begin{cases} \dot{y}_1 = a(y_2 - y_1) + y_3 y_2, \\ \dot{y}_2 = -y_2 - y_1 y_3 + b y_1, \\ \dot{y}_3 = -y_3 + y_1 y_2, \end{cases} \tag{4}$$

where a=5.45 and b=20 with initial condition (0.2, 0.2, 0.2). Figure 2 displays the chaotic attractor of PMSG system.

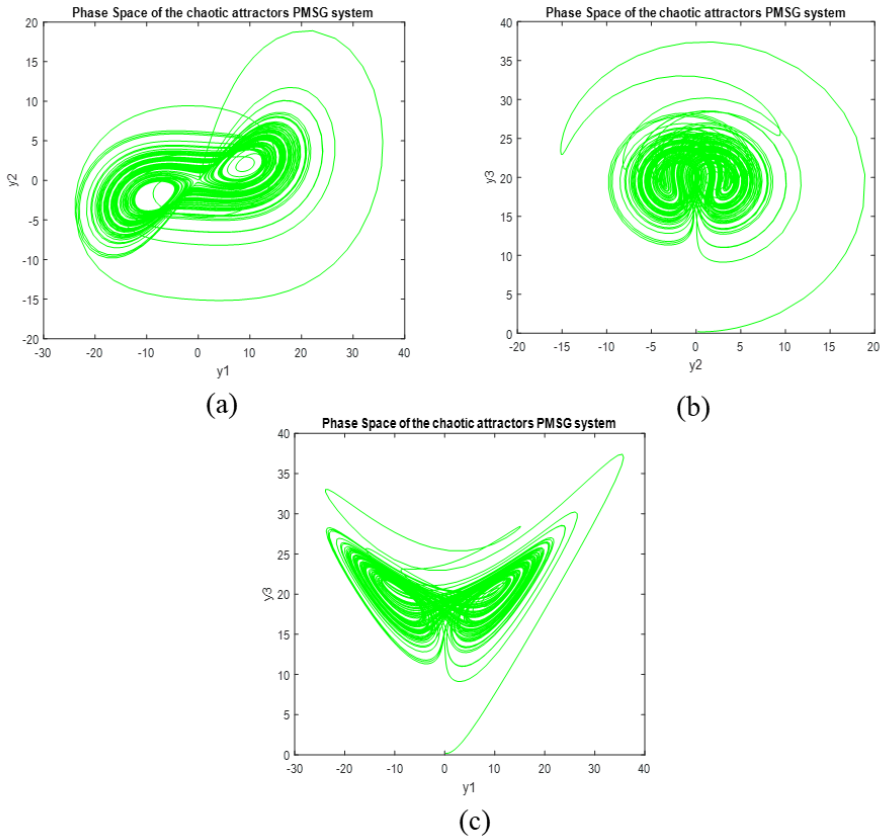

Figure 2. The chaotic attractors PSMG for (a) y_1-y_2, (b) y_2-y_3, and (c) y_1-y_3 planes using MATLAB.

Using MATLAB, the following is how we calculate the Lyapunov exponents of model (4) [31]:

$$LE_1 = 1.0154,\ LE_2 = -0.0003,\ LE_3 = -8.4651. \tag{5}$$

The Kaplan-Yorke dimension of system (2.4) is computed as follows:

$$D_{KY} = 2 + \frac{LE_1 + LE_2}{|LE_3|} = 2.119, \tag{6}$$

which points to the high level of complexity of the new system (4).

3. Dynamical analysis

3.1. Bifurcation diagram and Lyapunov exponent

The Lyapunov spectrum and bifurcation diagrams are respectively presented in Figures 3(a) and 3(b) by varying parameter a such that a ϵ [2, 18]. They indicate that the PMSG system (4) can generate periodic behavior and exhibit chaotic behavior. The system has periodic behavior in b ϵ ([2, 3.7], [4.35, 4.62], [12.2, 12.72], [15, 18]), and chaotic behavior in b ϵ ([3.7, 4.35], [4.62, 12.2], [12.72, 15]).

The Lyapunov exponent spectrum and bifurcation diagram of (4) are displayed in Figures 4(a) and 4(b), respectively. They indicate that the PMSG system (4) can generate stable behavior, periodic behavior and exhibit chaotic behavior. The system has stable behavior in b ϵ ([0, 5.2]), periodic behavior in b ϵ ([24.1, 25.6], [31.45, 50]), and chaotic behavior in b ϵ ([5.2, 24.1], [25.6, 31.45]).

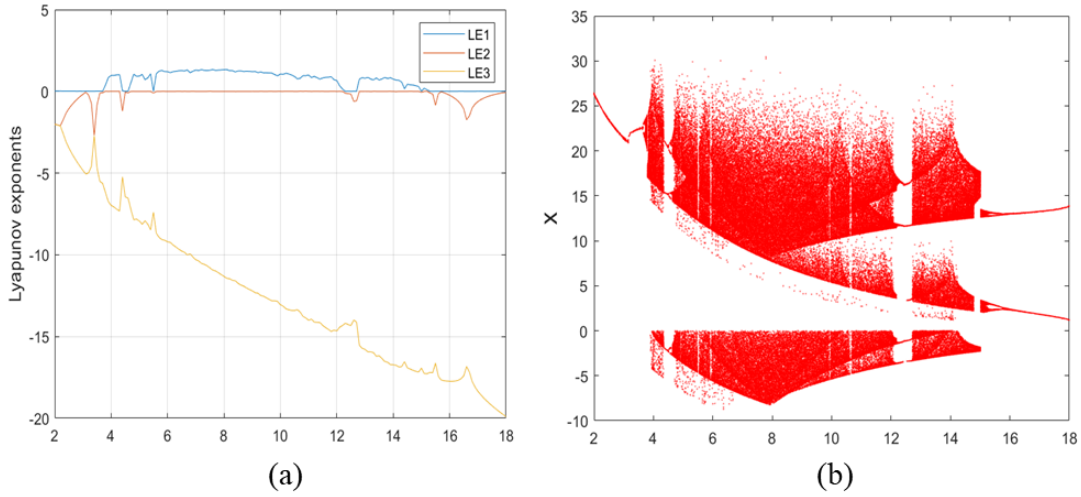

Figure 3. Dynamic analysis of the PMSG system (4) with parameter a varying and b=20; (a) Lyapunov exponents spectrum and (b) Bifurcation diagram.

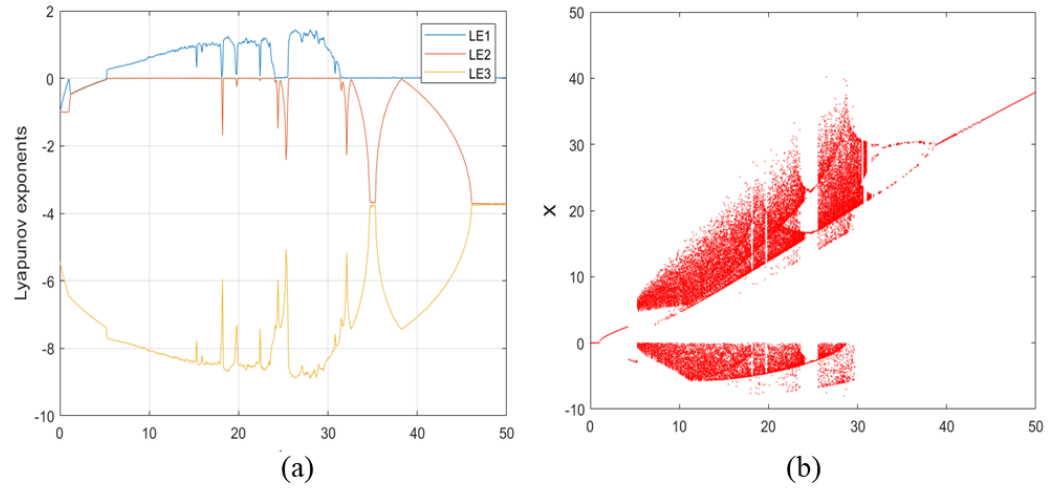

Figure 4. Dynamic analysis of the PMSG system (4) with parameter b varying and a=5.45; (a) Lyapunov exponents spectrum and (b) Bifurcation diagram.

3.2. Poincare map

Poincaré map is a fundamental and useful tool for learning about periodic state and its associated properties [32, 33]. It transforms a dynamical system with continuous time into one with discrete time, and converts the study of the flow in the vicinity of a closed orbit or a periodic solution into the study of a map [34–36]. The Poincaré map of (4) is presented in Figure 5. The diagram show that the Poincaré map exhibits chaotic behavior with densely packed trajectories.

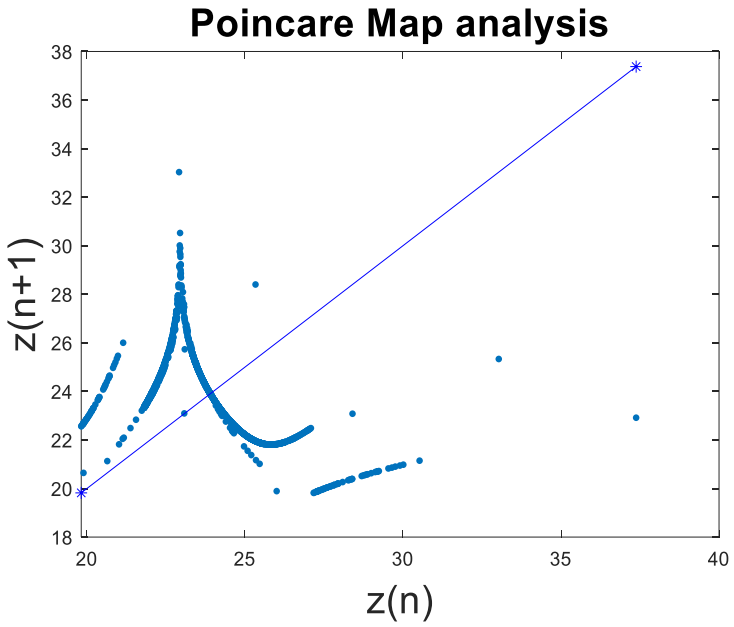

Figure 5. Poincaré map analysis of the PMSG system (4) with parameter a=5.45 and b=20.

4. Adaptive type-2 fuzzy controller

To design the controller, the dynamics of (4) are rewritten as:

$$\begin{cases} \dot{y}_1 = F_1(y) + u_1 \\ \dot{y}_2 = F_2(y) + u_2, \\ \dot{y}_3 = F_3(y) + u_3 \end{cases} \tag{7}$$

where,

$$F_1(y) = a(y_2 - y_1) + y_3 y_2,\ F_2(y) = -y_2 - y_1 y_3 + b y_1, F_3(y) = -y_3 + y_1 y_2, \tag{8}$$

with $y^T = [y_1, y_2, y_3]$, and $F_i(y),\ i = 1,2,3$ representing unknown functions approximated by suggested type-2 fuzzy logic systems (T2-FLSs) as $\hat{F}_i(y, \psi_i), i = 1,2,3$, where ψ_i denotes the rule parameters. The proposed controllers are:

$$\begin{cases} u_1 = -\hat{F}_1(y, \psi_1) + \dot{r}_1 - \kappa_1 \chi_1 \\ u_2 = -\hat{F}_2(y, \psi_2) + \dot{r}_2 - \kappa_2 \chi_2, \\ u_3 = -\hat{F}_3(y, \psi_3) + \dot{r}_3 - \kappa_3 \chi_3 \end{cases} \tag{9}$$

where, r_i represents the reference, χ_i is defined as $\chi_i = y_i - r_i$, and κ_i is a constant. By applying the controllers (9) on the system (7), we have

$$\begin{cases} \dot{\chi}_1 = F_1(y) - \hat{F}_1(y, \psi_1) - \kappa_1 \chi_1 \\ \dot{\chi}_2 = F_2(y) - \hat{F}_2(y, \psi_2) - \kappa_2 \chi_2. \\ \dot{\chi}_3 = F_3(y) - \hat{F}_3(y, \psi_3) - \kappa_3 \chi_3 \end{cases} \tag{10}$$

By considering the optimal $\hat{F}_i^*(y, \psi_1^*)$, we get:

$$\begin{cases} \dot{\chi}_1 = F_1(y) - \hat{F}_1^*(y, \psi_1^*) + \hat{F}_1^*(y, \psi_1^*) - \hat{F}_1(y, \psi_1) - \kappa_1 \chi_1 \\ \dot{\chi}_2 = F_2(y) - \hat{F}_2^*(y, \psi_2^*) + \hat{F}_2^*(y, \psi_2^*) - \hat{F}_2(y, \psi_2) - \kappa_2 \chi_2, \\ \dot{\chi}_3 = F_3(y) - \hat{F}_3^*(y, \psi_3^*) + \hat{F}_3^*(y, \psi_3^*) - \hat{F}_3(y, \psi_3) - \kappa_3 \chi_3 \end{cases} \tag{11}$$

also, by considering the following definition:

$$\begin{cases} \vartheta_1 = F_1(y) - \hat{F}_1^*(y, \psi_1^*) \\ \vartheta_2 = F_2(y) - \hat{F}_2^*(y, \psi_2^*), \\ \vartheta_3 = F_3(y) - \hat{F}_3^*(y, \psi_3^*) \end{cases} \tag{12}$$

then from (10), we obtain:

$$\begin{cases} \dot{\chi}_1 = \vartheta_1 + \hat{F}_1^*(y, \psi_1^*) - \hat{F}_1(y, \psi_1) - \kappa_1 \chi_1 \\ \dot{\chi}_2 = \vartheta_2 + \hat{F}_2^*(y, \psi_2^*) - \hat{F}_2(y, \psi_2) - \kappa_2 \chi_2, \\ \dot{\chi}_3 = \vartheta_3 + \hat{F}_3^*(y, \psi_3^*) - \hat{F}_3(y, \psi_3) - \kappa_3 \chi_3 \end{cases} \tag{13}$$

where term $\hat{F}_i^*(y, \psi_i^*) - \hat{F}_i(y, \psi_i)$ is rewritten as:

$$\hat{F}_i^*(y, \psi_i^*) - \hat{F}_i(y, \psi_i) = \tilde{\psi}_i^T \phi_i(y), \tag{14}$$

with, $\phi_i(y)$ defining the vector of normalized rule firing, and $\tilde{\psi}_i$ is defined as

$$\tilde{\psi}_i = \psi_i^* - \psi_i. \tag{15}$$

From (14), the Eq (13) becomes:

$$\begin{cases} \dot{\chi}_1 = \vartheta_1 + \tilde{\psi}_1^T \phi_1(y) - \kappa_1 \chi_1 \\ \dot{\chi}_2 = \vartheta_2 + \tilde{\psi}_2^T \phi_2(y) - \kappa_2 \chi_2. \\ \dot{\chi}_3 = \vartheta_3 + \tilde{\psi}_3^T \phi_3(y) - \kappa_3 \chi_3 \end{cases} \tag{16}$$

To extract the learning rules of T2-FLS, and ensure stability, consider Lyapunov as:

$$V = \frac{1}{2}\chi_1^2 + \frac{1}{2}\chi_2^2 + \frac{1}{2}\chi_3^2 + \frac{1}{2\lambda}\tilde{\psi}_1^T\tilde{\psi}_1 + \frac{1}{2\lambda}\tilde{\psi}_3^T\tilde{\psi}_2 + \frac{1}{2\lambda}\tilde{\psi}_3^T\tilde{\psi}_3, \tag{17}$$

where, λ is a constant. From (17), we have

$$\dot{V} = \chi_1\dot{\chi}_1 + \chi_2\dot{\chi}_2 + \chi_3\dot{\chi}_3 - \frac{1}{\lambda}\tilde{\psi}_1^T\dot{\psi}_1 - \frac{1}{\lambda}\tilde{\psi}_2^T\dot{\psi}_2 - \frac{1}{\lambda}\tilde{\psi}_3^T\dot{\psi}_3. \tag{18}$$

By substituting form (16), we have

$$\dot{V} = \chi_1\left(\vartheta_1 + \tilde{\psi}_1^T\phi_1(y) - \kappa_1\chi_1\right) + \chi_2\left(\vartheta_2 + \tilde{\psi}_2^T\phi_2(y) - \kappa_2\chi_2\right)$$
$$+\chi_3\left(\vartheta_3 + \tilde{\psi}_3^T\phi_3(y) - \kappa_3\chi_3\right) - \frac{1}{\lambda}\tilde{\psi}_1^T\dot{\psi}_1 - \frac{1}{\lambda}\tilde{\psi}_2^T\dot{\psi}_2 - \frac{1}{\lambda}\tilde{\psi}_3^T\dot{\psi}_3. \quad (19)$$

From (19), we have

$$\dot{V} = -\kappa_1\chi_1^2 - \kappa_2\chi_2^2 - \kappa_3\chi_3^2 + \chi_1\vartheta_1 + \chi_2\vartheta_2 + \chi_3\vartheta_3 + \tilde{\psi}_1^T\left(\chi_1\phi_1(y) - \frac{1}{\lambda}\dot{\psi}_1\right)$$
$$+\tilde{\psi}_2^T\left(\chi_2\phi_2(y) - \frac{1}{\lambda}\dot{\psi}_2\right) + \tilde{\psi}_3^T\left(\chi_3\phi_3(y) - \frac{1}{\lambda}\dot{\psi}_3\right) \quad (20)$$

From (20), the learning rules are considered as:

$$\dot{\psi}_1 = \lambda\chi_1\phi_1(y),\ \dot{\psi}_2 = \lambda\chi_2\phi_2(y),\ \dot{\psi}_3 = \lambda\chi_3\phi_3(y). \quad (21)$$

Then from (21), the Lyapunov function in (20), becomes

$$\dot{V} = -\kappa_1\chi_1^2 - \kappa_2\chi_2^2 - \kappa_3\chi_3^2 + \chi_1\vartheta_1 + \chi_2\vartheta_2 + \chi_3\vartheta_3. \quad (22)$$

From Eq (22), and considering the fact that

$$\begin{cases}\chi_i\vartheta_i \le |\chi_i||\vartheta_i| if |\chi_i| < 1\\ \chi_i\vartheta_i \le \chi_i^2|\vartheta_i| if |\chi_i| \ge 1\end{cases},$$

we can write:

$$\begin{cases}\dot{V} \le -\kappa_1|\chi_1| - \kappa_2|\chi_2| - \kappa_3|\chi_3| \\ +|\chi_1||\vartheta_1| + |\chi_2||\vartheta_2| + |\chi_3||\vartheta_3| if |\chi_i| < 1\\ \\ \dot{V} \le -\kappa_1\chi_1^2 - \kappa_2\chi_2^2 - \kappa_3\chi_3^2 \\ +\chi_1^2|\vartheta_1| + \chi_2^2|\vartheta_2| + \chi_3^2|\vartheta_3| if |\chi_i| \ge 1\end{cases} \quad (23)$$

Then by considering the feedback gains κ_i, the stability is ensured. The main point is that, by the use of T2-FLSs, the errors $\vartheta_i, i = 1,2,3$ are much small in comparison with type-1 counterparts. It should be noted that $\kappa_i, i = 1,2,3$ are positive constants. The larger values of $\kappa_i, i = 1,2,3$ increase the speed of convergence but leads to a bigger control signal. Then is choosing of $\kappa_i, i = 1,2,3$ a trade-off should be made between speed of convergence and magnitude of control signal. Also, the big $\kappa_i, i = 1,2,3$ help for stability. The values of $\kappa_i,\ i = 1,2,3$ should be bigger than $|\vartheta_i|$.

5. Simulation

The simulations in this study were conducted on Matlab programming software so as to assess the efficacy of the suggested approach. The designed controller is implemented in Matlab as shown in Figures 6–8. By considering the references as $sin(t) + cos(t)$, $cos(t)$, and $sin(t)$. Figures 9 and 10 gives the tracking response and tracking error. It can be seen that tracking error converted to small neighborhood around zero, expeditiously. Simulation results confirm that our proposed controller can guarantee the stability and robustness of the close loop system. Figure 11 show that the control signal

for the chaotic PMSG based on the conversion system of wind energy. Finally, Figure 12 present the phase portrait after designed controller to remove the chaotic PMSG wind turbine model.

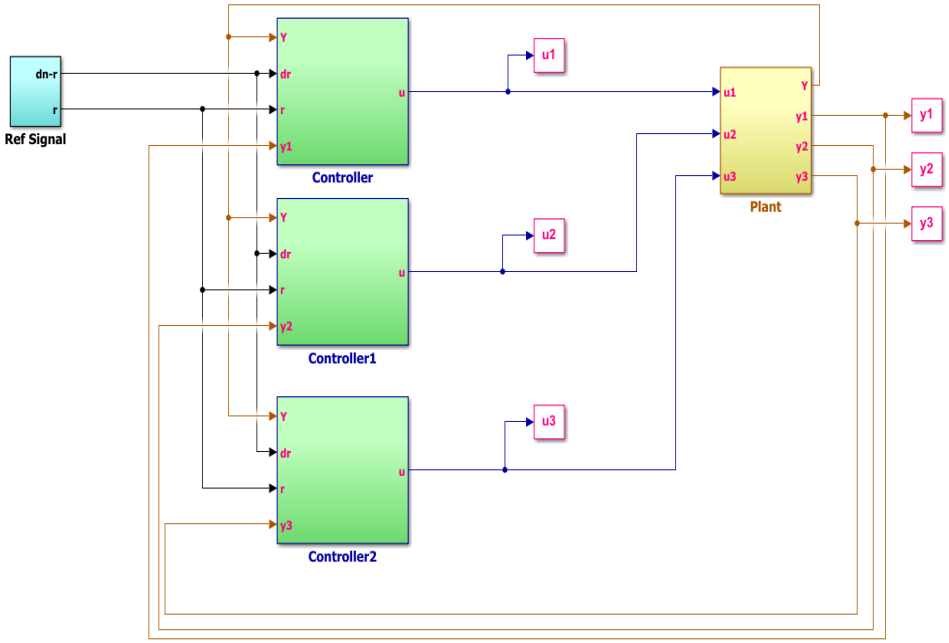

Figure 6. The general scheme of implemented controller.

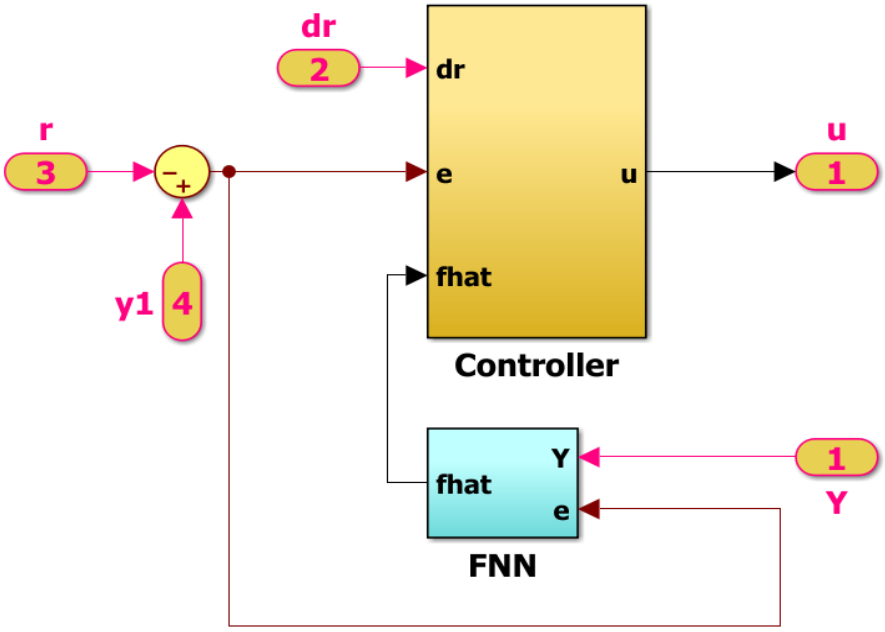

Figure 7. The MATLAB scheme of controller.

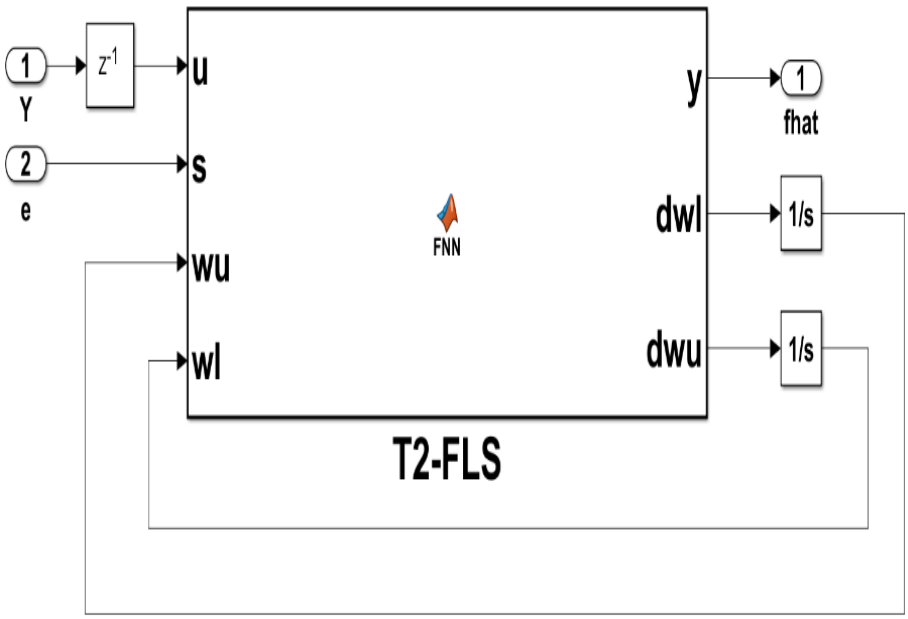

Figure 8. The implemented scheme of T2-FLS.

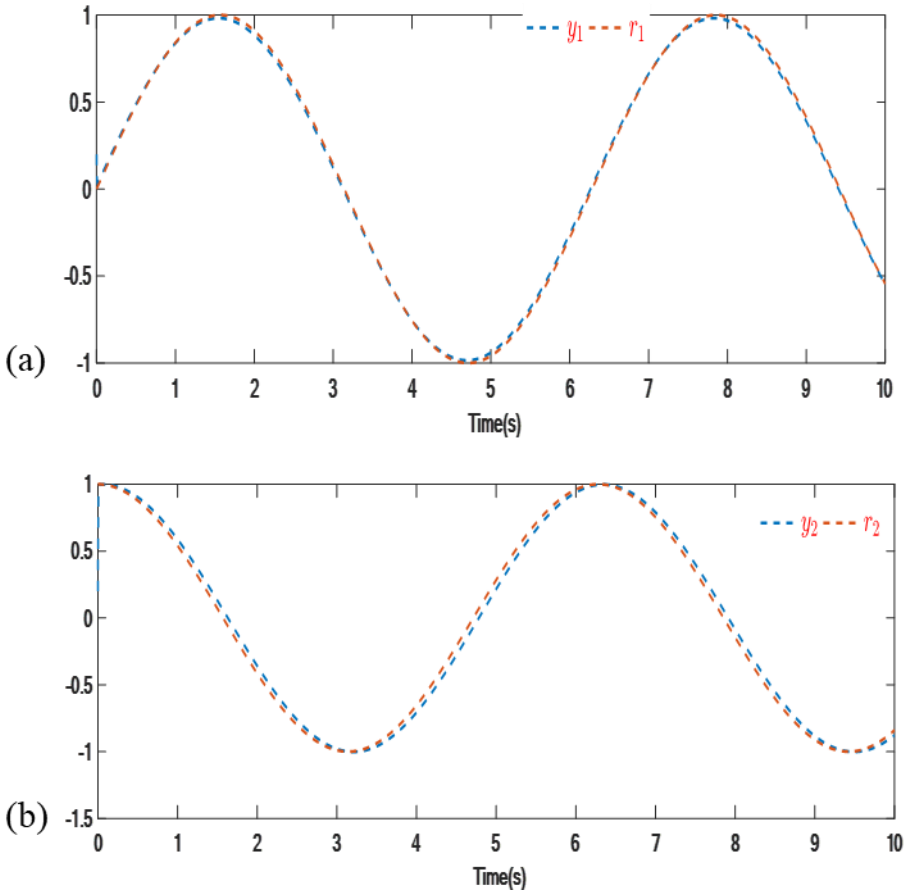

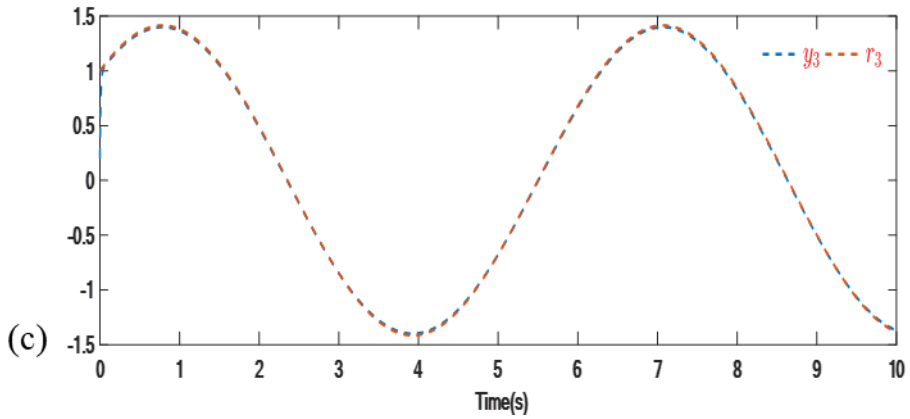

Figure 9. Numerical simulation using Matlab (a) Output trajectory y_1, (b) Output trajectory y_2, and (c) Output trajectory y_3.

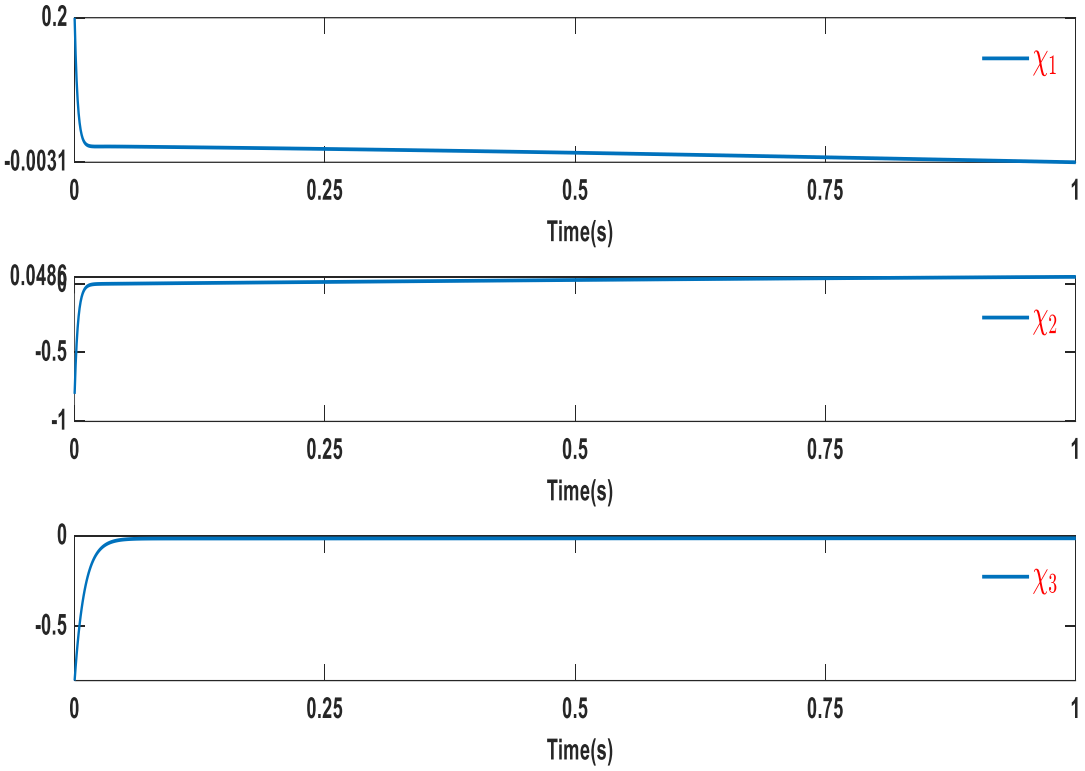

Figure 10. Tracking error.

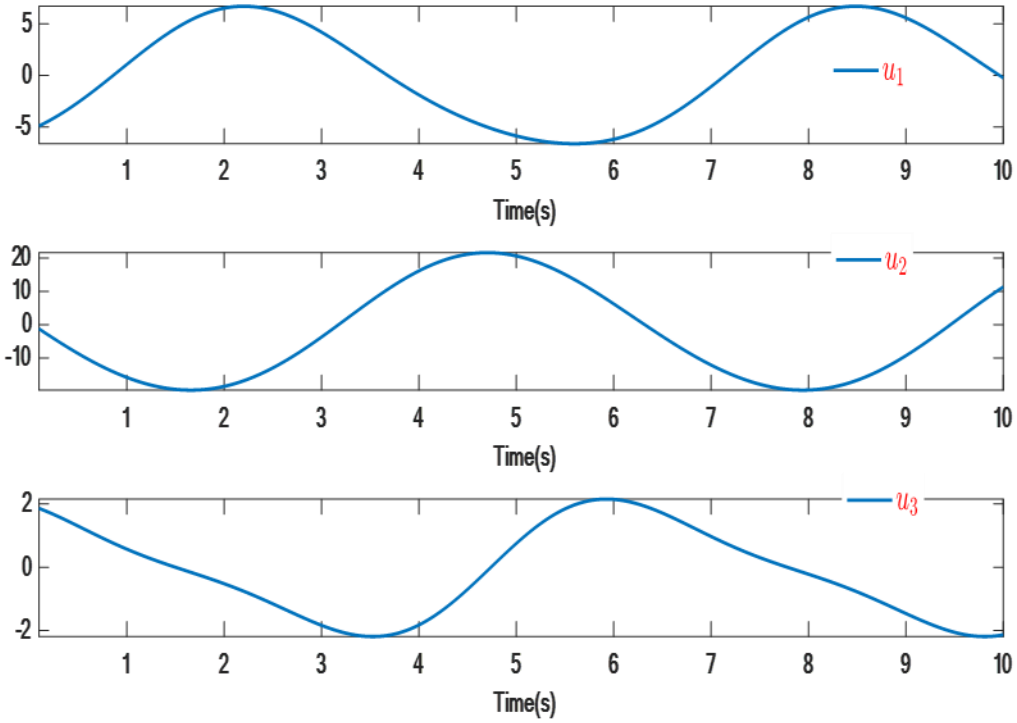

Figure 11. Control signals.

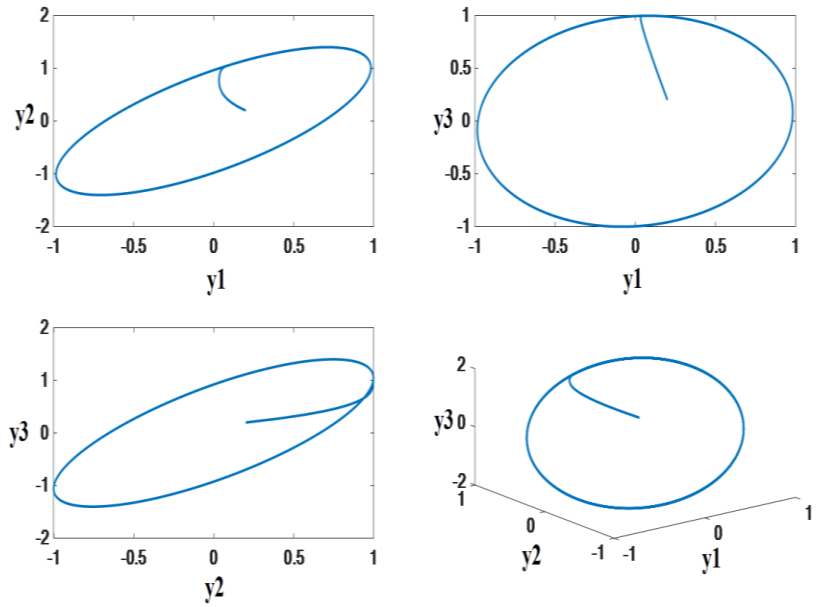

Figure 12. Phase Potrait using Matlab.

The performance of the proposed control method is compared with the Fuzzy PID control and Adaptive fuzzy control in terms of the root mean square (RMS) as presented in Table 1. On these bases,

it is concluded that the proposed controller outperforms the benchmarking techniques. In order to determine the robustness of the proposed control method, the simulations are further carried out under different longitudinal velocities, and matched uncertainties.

Table 1. Root mean square error comparison.

Methods	Error signals		
	χ_1	χ_2	χ_3
Proposed	0.0124	0.2511	1.1204
Fuzzy PID [37]	0.0132	0.3612	3.0172
Adaptive fuzzy controller [38]	0.0114	0.5417	6.4120

6. Conclusions

In this article, we investigated the chaotic behavior of Permanent Magnet Synchronous Generator (PMSG) in a wind turbine system with quadratic nonlinearities. The bifurcation diagrams, Lyapunov exponents, Poincare maps, and Phase portraits, have all been used to illustrate the intricate dynamical characteristics of PMSG chaotic system. Finally, an adaptive type-2 fuzzy controller is designed for different flow configurations of the PMSG. To further demonstrate the effectiveness of the proposed approach, we presented analysis of the performance by simulating the PMSG. This simulation study of the PMSG guarantees the efficiency and performance of the new procedure.

Acknowledgments

Aceng Sambas appreciates the Postdoctoral Fellowship from Universiti Malaysia Terengganu (UMT), Mohamad Afendee Mohamed was partially funded by CREIM, Universiti Sultan Zainal Abidin (UniSZA) and Mohamad Arif Awang Nawi was partially funded with grant Number: 304/PPSG/6315410.

Conflict of interest

The authors declare no conflict of interest.

References

1. J. D. Li, G. D. Wang, Z. H. Li, S. L. Yang, W. T. Chong, X. B. Xiang, A review on development of offshore wind energy conversion system, *Int. J. Energy Res.*, **44** (2020), 9283–9297. https://doi.org/10.1002/er.5751
2. K. B. Tawfiq, A. S. Mansour, H. S. Ramadan, M. Becherif, E. E. El-Kholy, Wind energy conversion system topologies and converters: Comparative review, *Energy Procedia*, **162** (2019), 38–47. https://doi.org/10.1016/j.egypro.2019.04.005
3. Z. Q. Wu, W. J. Jia, L. R. Zhao, C. H. Wu, Maximum wind power tracking for PMSG chaos systems-ADHDP method, *Appl. Soft Comput.*, **36** (2015), 204–209. https://doi.org/10.1016/j.asoc.2015.07.024

4. M. Borah, B. K. Roy, Dynamics of the fractional-order chaotic PMSG, its stabilisation using predictive control and circuit validation, *IET Electri. Power Appl.*, **11** (2017), 707–716. https://doi.org/10.1049/iet-epa.2016.0506
5. N. K. Saxena, A. Kumar, V. Gupta, Enhancement of system performance using STATCOM as dynamic compensator with squirrel cage induction generator (SCIG) based microgrid, *Int. J. Emerg. Electri. Power Syst.*, **22** (2021), 177–189. https://doi.org/10.1515/ijeeps-2020-0228
6. P. Raja, M. P. Selvan, N. Kumaresan, Enhancement of voltage stability margin in radial distribution system with squirrel cage induction generator based distributed generators, *IET Gener. Transm. Dis.*, **7** (2013), 898–906. https://doi.org/10.1049/iet-gtd.2012.0579
7. C. Kalaivani, K. Rajambal, Modeling and analysis of multiphase induction generator, In: *2016 International conference on circuit, power and computing technologies*, 2016. https://doi.org/10.1109/ICCPCT.2016.7530363
8. K. Chandramohan, S. Padmanaban, R. Kalyanasundaram, F. Blaabjerg, Modeling of five-phase, self-excited induction generator for wind mill application, *Electri. Power Compo. Syst.*, **46** (2018), 353–363. https://doi.org/10.1080/15325008.2018.1444689
9. W. L. Dai, Y. H. Yu, M. Hua, C. C. Cai, Voltage regulation system of doubly salient electromagnetic generator based on indirect adaptive fuzzy control, *IEEE Access*, **5** (2017), 14187–14194. https://doi.org/10.1109/ACCESS.2017.2719048
10. Y. Zhao, H. Z. Wang, L. Xiao, Investigation of fault-tolerant capability of five-phase doubly salient electromagnetic generator, *IET Electri. Power Appl.*, **9** (2015), 80–93. https://doi.org/10.1049/iet-epa.2014.0058
11. B. H. Chowdhury, S. Chellapilla, Double-fed induction generator control for variable speed wind power generation, *Electri. Power Syst. Res.*, **76** (2006), 786–800. https://doi.org/10.1016/j.epsr.2005.10.013
12. J. B. Ekanayake, L. Holdsworth, X. G. Wu, N. Jenkins, Dynamic modeling of doubly fed induction generator wind turbines, *IEEE Trans. Power Syst.*, **18** (2003), 803–809. https://doi.org/10.1109/TPWRS.2003.811178
13. N. Hiron, N. Busaeri, S. Sutisna, N. Nurmela, A. Sambas, Design of hybrid (PV-Diesel) system for tourist island in Karimunjawa Indonesia, *Energies*, **14** (2021), 8311. https://doi.org/10.3390/en14248311
14. A. Dahbi, M. Hachemi, N. Nait-Said, M. S. Nait-Said, Realization and control of a wind turbine connected to the grid by using PMSG, *Energy Convers. Manage.*, **84** (2014), 346–353. https://doi.org/10.1016/j.enconman.2014.03.085
15. A. Jain, S. Shankar, V. Vanitha, Power generation using permanent magnet synchronous generator (PMSG) based variable speed wind energy conversion system (WECS): An overview, *J. Green Eng.*, **7** (2017), 477–504. https://doi.org/10.13052/jge1904-4720.742
16. N. A. Orlando, M. Liserre, R. A. Mastromauro, A. Dell'Aquila, A survey of control issues in PMSG-based small wind-turbine systems, *IEEE Tran. Ind. Inform.*, **9** (2013), 1211–1221. https://doi.org/10.1109/TII.2013.2272888
17. K. Tan, S. Islam, Optimum control strategies in energy conversion of PMSG wind turbine system without mechanical sensors, *IEEE Tran. Energy Convers.*, **19** (2004), 392–399. https://doi.org/10.1109/TEC.2004.827038
18. H. W. Kim, S. S. Kim, H. S. Ko, Modeling and control of PMSG-based variable-speed wind turbine, *Electri. Power Syst. Res.*, **80** (2010), 46–52. https://doi.org/10.1016/j.epsr.2009.08.003

19. M. Mansour, M. N. Mansouri, S. Bendoukha, M. F. Mimouni, A grid-connected variable-speed wind generator driving a fuzzy-controlled PMSG and associated to a flywheel energy storage system, *Electri. Power Syst. Res.*, **180** (2020), 106137. https://doi.org/10.1016/j.epsr.2019.106137
20. A. Honarbari, S. Najafi-Shad, M. S. Pour, S. S. M. Ajarostaghi, A. Hassannia, MPPT improvement for PMSG-based wind turbines using extended Kalman filter and fuzzy control system, *Energies*, **14** (2021), 7503. https://doi.org/10.3390/en14227503
21. L. Z. Ren, T. F. Lei, H. Chen, R. Wang, Optimal control research for the wind turbine PMSG chaos motion, *Appl. Mech. Mater.*, **543** (2014), 1291–1295. https://doi.org/10.4028/www.scientific.net/AMM.543-547.1291
22. M. Messadi, A. Mellit, K. Kemih, M. Ghanes, Predictive control of a chaotic permanent magnet synchronous generator in a wind turbine system, *Chinese Phys. B*, **24** (2015), 010502. https://doi.org/10.1088/1674-1056/24/1/010502
23. G. Q. Si, J. W. Zhu, L. J. Diao, Z. Q. Ding, Modeling, nonlinear dynamic analysis and control of fractional PMSG of wind turbine, *Nonlinear Dyna.*, **88** (2017), 985–1000. https://doi.org/10.1007/s11071-016-3289-9
24. G. A. Alamdar, S. Balochian, Chaos control of permanent magnet synchronous generator via sliding mode controller, *Majlesi J. Electr. Eng.*, **13** (2019), 1–5.
25. X. C. Hu, S. H. Luo, L. Zhao, H. H. Ma, Adaptive backstepping control of the PMSG based on the T2SFNN, In: *2020 Chinese automation congress*, 2020. https://doi.org/10.1109/CAC51589.2020.9326471
26. S. Kahla, M. Bechouat, T. Amieur, M. Sedraoui, B. Babes, N. Hamouda, Maximum power extraction framework using robust fractional-order feedback linearization control and GM-CPSO for PMSG-based WECS, *Wind Eng.*, **45** (2021), 1040–1054. https://doi.org/10.1177/0309524X20948263
27. S. H. Luo, X. Ch. Hu, L. Zhao, S. B. Li, Event-triggered neural adaptive backstepping control of the K chaotic PMSGs coupled system, *Internat, J. Electr. Power Energy Syst.*, **135** (2022), 107475. https://doi.org/10.1016/j.ijepes.2021.107475
28. H. Takhi, L. Moysis, N. Machkour, C. Volos, K. Kemih, M. Ghanes, Predictive control and synchronization of uncertain perturbed chaotic permanent-magnet synchronous generator and its microcontroller implementation, *Eur. Phys. J. Spec. Top.*, **231** (2022), 443–451. https://doi.org/10.1140/epjs/s11734-021-00422-4
29. E. H. Dursun, H. Koyuncu, A. A. Kulaksiz, A novel unified maximum power extraction framework for PMSG based WECS using chaotic particle swarm optimization derivatives, *Eng. Sci. Technol. Int. J.*, **24** (2021), 158–170. https://doi.org/10.1016/j.jestch.2020.05.005
30. L. Shanmugam, Y. H. Joo, Stabilization of permanent magnet synchronous generator-based wind turbine system via fuzzy-based sampled-data control approach, *Inform. Sci.*, **559** (2021), 270–285. https://doi.org/10.1016/j.ins.2020.12.088
31. A. Wolf, J. B. Swift, H. L. Swinney, J. A. Vastano, Determining Lyapunov exponents from a time series, *Phys. D*, **16** (1985), 285–317. https://doi.org/10.1016/0167-2789(85)90011-9
32. H. Gritli, S. Belghith, Walking dynamics of the passive compass-gait model under OGY-based state-feedback control: Analysis of local bifurcations via the hybrid Poincaré map, *Chaos, Solitons Fractals*, **98** (2017), 72–87. https://doi.org/10.1016/j.chaos.2017.03.004

33. D. Clemente-López, E. Tlelo-Cuautle, L. G. de la Fraga, J. de Jesús Rangel-Magdaleno, J. M. Munoz-Pacheco, Poincaré maps for detecting chaos in fractional-order systems with hidden attractors for its Kaplan-Yorke dimension optimization, *AIMS Mathematics*, **7** (2022), 5871–5894. https://doi.org/10.3934/math.2022326
34. S. Vaidyanathan, A. Sambas, E. Tlelo-Cuautle, A. A. Abd El-Latif, B. Abd-El-Atty, O. Guillén-Fernández, et al., A new 4-D multi-stable hyperchaotic system with no balance point: Bifurcation analysis, circuit simulation, FPGA realization and image cryptosystem, *IEEE Access*, **9** (2021), 144555–144573. https://doi.org/10.1109/ACCESS.2021.3121428
35. K. Benkouider, T. Bouden, A. Sambas, M. A. Mohamed, I. M. Sulaiman, M. Mamat, et al., Dynamics, control and secure transmission electronic circuit implementation of a new 3D chaotic system in comparison with 50 reported systems, *IEEE Access*, **9** (2021), 152150–152168. https://doi.org/10.1109/ACCESS.2021.3126655
36. A. Sambas, M. Mamat, S. Vaidyanathan, M. Mohamed, M. Sanjaya, A new 4-D chaotic system with hidden attractor and its circuit implementation, *Int. J. Eng. Technol.*, **7** (2018), 1245–1250. https://doi.org/10.14419/ijet.v7i3.9846
37. J. Tavoosi, M. Shirkhani, A. Abdali, A. Mohammadzadeh, M. Nazari, S. Mobayen, et al., A new general type-2 fuzzy predictive scheme for PID tuning, *Appl. Sci.*, **11** (2021), 10392. https://doi.org/10.3390/app112110392
38. A. Mohammadzadeh, H. Taghavifar, A novel adaptive control approach for path tracking control of autonomous vehicles subject to uncertain dynamics, *Proc. Inst. Mech. Eng. D-J. Aut. Eng.*, **234** (2020), 2115–2126. https://doi.org/10.1177/0954407019901083

AIMS Press